Calhoun: The NPS Institutional Archive

DSpace Repository

Theses and Dissertations | 1. Thesis and Dissertation Collection, all items

2019-12

INVESTIGATION OF ATMOSPHERIC ENVIRONMENTS CONDUCIVE TO SUPERCELL TRANSFORMATION INTO A MESOSCALE CONVECTIVE SYSTEM

Youngblood, Alanna

Monterey, CA; Naval Postgraduate School

http://hdl.handle.net/10945/64104

Downloaded from NPS Archive: Calhoun

http://www.nps.edu/library

Calhoun is a project of the Dudley Knox Library at NPS, furthering the precepts and goals of open government and government transparency. All information contained herein has been approved for release by the NPS Public Affairs Officer.

Dudley Knox Library / Naval Postgraduate School
411 Dyer Road / 1 University Circle
Monterey, California USA 93943

NAVAL POSTGRADUATE SCHOOL

MONTEREY, CALIFORNIA

THESIS

INVESTIGATION OF ATMOSPHERIC ENVIRONMENTS CONDUCIVE TO SUPERCELL TRANSFORMATION INTO A MESOSCALE CONVECTIVE SYSTEM

by

Alanna Youngblood

December 2019

Thesis Advisor: John M. Peters
Second Reader: Joel W. Feldmeier

Approved for public release. Distribution is unlimited.

THIS PAGE INTENTIONALLY LEFT BLANK

REPORT DOCUMENTATION PAGE			*Form Approved OMB No. 0704-0188*

Public reporting burden for this collection of information is estimated to average 1 hour per response, including the time for reviewing instruction, searching existing data sources, gathering and maintaining the data needed, and completing and reviewing the collection of information. Send comments regarding this burden estimate or any other aspect of this collection of information, including suggestions for reducing this burden, to Washington headquarters Services, Directorate for Information Operations and Reports, 1215 Jefferson Davis Highway, Suite 1204, Arlington, VA 22202-4302, and to the Office of Management and Budget, Paperwork Reduction Project (0704-0188) Washington, DC 20503.

1. AGENCY USE ONLY *(Leave blank)*	**2. REPORT DATE** December 2019	**3. REPORT TYPE AND DATES COVERED** Master's thesis

4. TITLE AND SUBTITLE
INVESTIGATION OF ATMOSPHERIC ENVIRONMENTS CONDUCIVE TO SUPERCELL TRANSFORMATION INTO A MESOSCALE CONVECTIVE SYSTEM

5. FUNDING NUMBERS

6. AUTHOR(S) Alanna Youngblood

7. PERFORMING ORGANIZATION NAME(S) AND ADDRESS(ES)
Naval Postgraduate School
Monterey, CA 93943-5000

8. PERFORMING ORGANIZATION REPORT NUMBER

9. SPONSORING / MONITORING AGENCY NAME(S) AND ADDRESS(ES)
N/A

10. SPONSORING / MONITORING AGENCY REPORT NUMBER

11. SUPPLEMENTARY NOTES The views expressed in this thesis are those of the author and do not reflect the official policy or position of the Department of Defense or the U.S. Government.

12a. DISTRIBUTION / AVAILABILITY STATEMENT	**12b. DISTRIBUTION CODE**
Approved for public release. Distribution is unlimited.	A

13. ABSTRACT (maximum 200 words)

The environmental factors that contribute to supercell thunderstorms transitioning into mesoscale convective systems (MCSs) are poorly understood. Numerous studies have investigated these phenomena separately, but few have studied the interconnected dynamics that cause a transition between supercells and MCSs. This lack of knowledge significantly affects the ability to forecast severe weather impacts associated with each system, such as severe lightning, wind, hail, flooding, and tornadoes. Previous studies highlight four specific elements needed for the formation of both supercells and MCSs: low-level vertical wind shear, upper-level vertical wind shear, convective available potential energy (CAPE), and relative humidity (RH). Using a high-resolution cloud model, multiple combinations of the aforementioned environmental factors were investigated to determine which distinct combination contributed to a supercell's initial development and MCS transition. Through data analysis focusing on areas of convectivity, potential temperature (theta) perturbations, and total mass flux, it was concluded that MCS growth from supercells is favored in environments with highest values of CAPE and RH, with low-level shear and upper-level shear inducing minor impacts. These results will facilitate refinement of MCS transition models.

14. SUBJECT TERMS	**15. NUMBER OF PAGES**
supercell, mesoscale convective system, MCS, MCSs, severe weather, tornado, tornadoes, supercell transition, mid-latitude severe weather	49
	16. PRICE CODE

17. SECURITY CLASSIFICATION OF REPORT	**18. SECURITY CLASSIFICATION OF THIS PAGE**	**19. SECURITY CLASSIFICATION OF ABSTRACT**	**20. LIMITATION OF ABSTRACT**
Unclassified	Unclassified	Unclassified	UU

NSN 7540-01-280-5500

Standard Form 298 (Rev. 2-89)
Prescribed by ANSI Std. 239-18

THIS PAGE INTENTIONALLY LEFT BLANK

Approved for public release. Distribution is unlimited.

INVESTIGATION OF ATMOSPHERIC ENVIRONMENTS CONDUCIVE TO SUPERCELL TRANSFORMATION INTO A MESOSCALE CONVECTIVE SYSTEM

Alanna Youngblood
Lieutenant Commander, United States Navy
BS, U.S. Naval Academy, 2009

Submitted in partial fulfillment of the
requirements for the degree of

MASTER OF SCIENCE IN METEOROLOGY AND PHYSICAL OCEANOGRAPHY

from the

NAVAL POSTGRADUATE SCHOOL
December 2019

Approved by: John M. Peters
Advisor

Joel W. Feldmeier
Second Reader

Wendell A. Nuss
Chair, Department of Meteorology

THIS PAGE INTENTIONALLY LEFT BLANK

ABSTRACT

The environmental factors that contribute to supercell thunderstorms transitioning into mesoscale convective systems (MCSs) are poorly understood. Numerous studies have investigated these phenomena separately, but few have studied the interconnected dynamics that cause a transition between supercells and MCSs. This lack of knowledge significantly affects the ability to forecast severe weather impacts associated with each system, such as severe lightning, wind, hail, flooding, and tornadoes. Previous studies highlight four specific elements needed for the formation of both supercells and MCSs: low-level vertical wind shear, upper-level vertical wind shear, convective available potential energy (CAPE), and relative humidity (RH). Using a high-resolution cloud model, multiple combinations of the aforementioned environmental factors were investigated to determine which distinct combination contributed to a supercell's initial development and MCS transition. Through data analysis focusing on areas of convectivity, potential temperature (theta) perturbations, and total mass flux, it was concluded that MCS growth from supercells is favored in environments with highest values of CAPE and RH, with low-level shear and upper-level shear inducing minor impacts. These results will facilitate refinement of MCS transition models.

THIS PAGE INTENTIONALLY LEFT BLANK

TABLE OF CONTENTS

THIS PAGE INTENTIONALLY LEFT BLANK

LIST OF FIGURES

THIS PAGE INTENTIONALLY LEFT BLANK

LIST OF TABLES

THIS PAGE INTENTIONALLY LEFT BLANK

ACKNOWLEDGMENTS

To my mom and dad for keeping me sane and my spirits high through this whole journey. I literally can't think of anyone with better parents in their lives! To my cohort, and Jen Gruber especially, for being my support through all the trials and tribulations that are the NPS experience. And to my local theater family, I never knew what I was missing before I met you amazing people. I couldn't have asked for a more supportive, loving, and all-encompassing group. Stay weird!

THIS PAGE INTENTIONALLY LEFT BLANK

I. INTRODUCTION

The United States is home to a wide range of high impact weather phenomena. Two of the most severe of these phenomena are supercell thunderstorms and Mesoscale Convective Systems (MCSs) (Gallus 2008). Paul Markowski (2007) references K. Brown's concept that a supercell thunderstorm was distinguishable as a unique storm type, and each consist of a solitary updraft with a rotating core. Markowski further categorized a supercell's rotating core as long-lasting, such that a single air parcel is able to travel the core's entire vertical length during the life of the storm. He also states that the horizontal span of the rotating core itself must be at least half of the originating storm's entire vertical extent. Markowski observed that most of these rotating core supercells had an average lifespan ranging approximately 1–4 hours. In contrast to supercells, J.M. Fritsch (2001) states that the term "MCS" is given to a particular weather phenomenon that is comprised of multiple individual thunderstorms, develops on a scale significantly larger than said individual updrafts (sometimes being large enough to be considered synoptic scale phenomena), and exists on time scales ranging 6–12 hours (or even longer).

Both MCSs and supercells present extensive risk to society. Supercell thunderstorms are associated with the production of destructive tornadoes, hailstones measured at a diameter of five inches or greater, the most intense lightning flash rates ever recorded (over 200 flashes per minute within an area 10 km^2 or less: Markowski 2007), damaging straight-line winds, microbursts, and heavy rainfall (Smith et al. 2001; Hitchens and Brooks 2013). MCSs, especially those that evolve from supercells, exhibit not only the severe weather phenomena associated with the originating supercell (especially within the immediate transformation phase; Fritsch and Forbes 2001), but also extreme rainfall rivaling that of a landfalling tropical cyclone (Fritsch et al. 1986), and widespread damaging winds due to the presence of rear inflow jets (Weisman 1992 and 1993). Several field study analyses concur that the peak rainfall rate within an MCS occurs within the development phase or roughly 2–6 hours after transition (Collander 1993; McAnelly and Cotton 1989). Additionally, it has been seen that for an MCS, the strong, damaging winds occur within the mature phase (Fritsch and Forbes 2001). Maddox (1980) observed that,

statistically, one in every five MCSs is responsible for a human death. MCSs are also so large in scale that they can affect and change the surrounding mesoscale to synoptic environment. Most importantly they can create persistent vorticity anomalies which can further contribute to the development of new MCSs (Fritsch and Forbes 2001).

The environments that spawn supercell thunderstorms and MCSs are very similar, and consequently MCSs often form from supercells (Fritsch and Forbes 2001). Supercells develop within environments of strong low-level wind shear which manifest as clockwise turning of wind direction with height within the first kilometer. This low-level wind curvature corresponds to ample streamwise vorticity and storm-relative helicity, which is responsible for low-level updraft rotation (Davies-Jones 1984; Weisman and Rotunno 2000; Thompson et. al 2003,2007,2012). Similarly, MCSs typically develop near the termination of strong low-level jets where strong vertical wind shear is present. Suitably strong ambient environmental shear allows for mechanical lifting to occur at outflow boundaries created by cold pools, as well as strong synoptic scale warm air advection in the lower levels (Fritsch and Forbes 2001; Coniglio et al. 2006, 2007, 2010; Peters and Schumacher 2014, 2015a, 2016). Other individual environmental factors such as convective available potential energy (CAPE) must also be present for the development of both supercells and MCSs, as this element is necessary for deep convection in general. Similarly, middle tropospheric relative humidity influences the strength of convective updrafts and potentially precipitation rates (Morrison 2016). However, previous studies have not pinned down the ranges of these variable that are favorable for MCS development (Rasmussen and Wilhelmson 1983). For instance, operational forecast parameters such as the Supercell Composite suggest a larger chance for sustained supercells with higher CAPE values (Thompson et al. 2003). However, other studies have shown that precipitation rates tend to correlate with CAPE, and the associated increase in cold pool production in higher CAPE environments may facilitate upscale growth (Gropp and Davenport 2018). Likewise, some studies suggest that low relative humidity promotes cold pool production (Proctor 1989); whereas, other studies show reduced cold pool production with low middle troposphere relative humidity (Grant and Van Den Heever 2014).

While supercell-to-MCS transitions are common, not all supercells transform into MCSs. Little is known about what specific environmental factors cause one supercell to transform into an MCS while another supercell simply decays without MCS development. The transition from supercell to MCS can be considered the most dangerous period since environmental impacts of both phenomena, i.e., tornadoes, hail, damaging winds, intense lightning storms, and flash flooding, can occur (e.g. Nielsen et al. 2015). Being able to distinguish the key factors which increase the probability of supercell thunderstorm transition will be incredibly beneficial to all early warning and resource protection programs.

This thesis highlights certain environmental components that, when present, will accurately forecast the supercell-to-MCS transition. Various cases involving different initial conditions were used to run simulations of convection using Cloud Model 1 (CM1). Low-level wind shear, deep-layer shear, CAPE, and RH values have been considered at different intensities to determine if any combination of these characteristics incite a transition from a supercell into an MCS. To address the uncertainty regarding the influence of CAPE on upscale growth, I hypothesize CAPE values, and not wind shear values, will be the deciding factor between environments where super cell thunderstorms complete the transition to an MCS and those that do not. Furthermore, that it is large CAPE values that increase the likelihood of a transition from a supercell into an MCS because large CAPE promotes greater vertical mass flux, precipitation production, and subsequent cold pool formation. The organization of this paper is as follows: a detailed description of CM1 including all domain parameters, control values and associated variations, additional characteristic values, and a detailed data analysis is contained in Chapter II; results and discussion are in Chapter III; summary and conclusion is in Chapter IV.

THIS PAGE INTENTIONALLY LEFT BLANK

II. METHODS

A. MODEL SETUP

Simulations were run using Cloud Model 1 (CM1; Bryan and Fritsch 2002), which is a three-dimensional, non-hydrostatic model designed to directly simulate clouds. CM1 typically uses a single sounding as initial and lateral boundary conditions with an added perturbation in the initial conditions to cause deep convection to develop. It is specifically designed to conserve total energy within a system to a higher order magnitude of accuracy than any other current model (NCAR 2019). Boundaries at the surface and top of the atmosphere were set as free slip, and radiation physics as well as fluxes between the surface and atmosphere were not considered. Microphysical processes were parameterized using the double moment scheme of Morrison et al. (2008) with hail as the prognostic rimed hydrometeor species. The model horizontal grid extent was set to 500 km in both the x- and y-directions. The model vertical grid extent was set to 18 km in the z-direction. Grid point spacings were set to 1 km in the horizontal and 100 m in the vertical. Various combinations of domain size and grid spacings were tested, and our results were insensitive to grid resolution. Output frequency was set to every 5 minutes. Coriolis acceleration affects were tested for any impacts to results and found to be insignificant at utilized length and times scales. Complete model setup information can be found in Table 1.

Table 1. Summary of the CM1 Configuration

Attribute	Value/Setting	Notes
Fully Compressible	Yes	
Horizontal Grid Spacing	1 km	
Vertical Grid Spacing	100 m	
Vertical Coordinate	Height (m)	
Number of x and y Points	500 x 500	
Vertical Points	180	
Top/Bottom LBCs	Free-slip	
North/South LBCs	Open-radiative	Durran and Klemp (2003)
East/West LBCs	Open-radiative	Durran and Klemp (1983)
Convection Initiation	Warm bubble at domain center, horizontal radius: 5 k, vertical radius: 1.4 km, theta perturbation: 3 K	
Microphysics	Morrison	Morrison et al. (2009)
Diffusion	6th Order	
Subgrid Turbulence	TKE	
Rayleigh Dampening	Yes	
Dissipative Heating	Yes	
2nd and 6th Order Coef.	75 - .04	
Longwave Radiation	None	
Shortwave Radiation	None	
Surface Layer	None	
Boundary Layer Physics	None	
Cumulus Parameterization	None	

B. INITIAL MODEL PROFILE

The initial or "control" thermodynamic profile used for all of the runs was the analytic profile given by Weisman and Klemp (1982), which will be hereafter referred as the WK82 sounding. Additionally, the wind profile shapes follow the "quarter circle" wind profile developed by Rotunno and Klemp (1982).

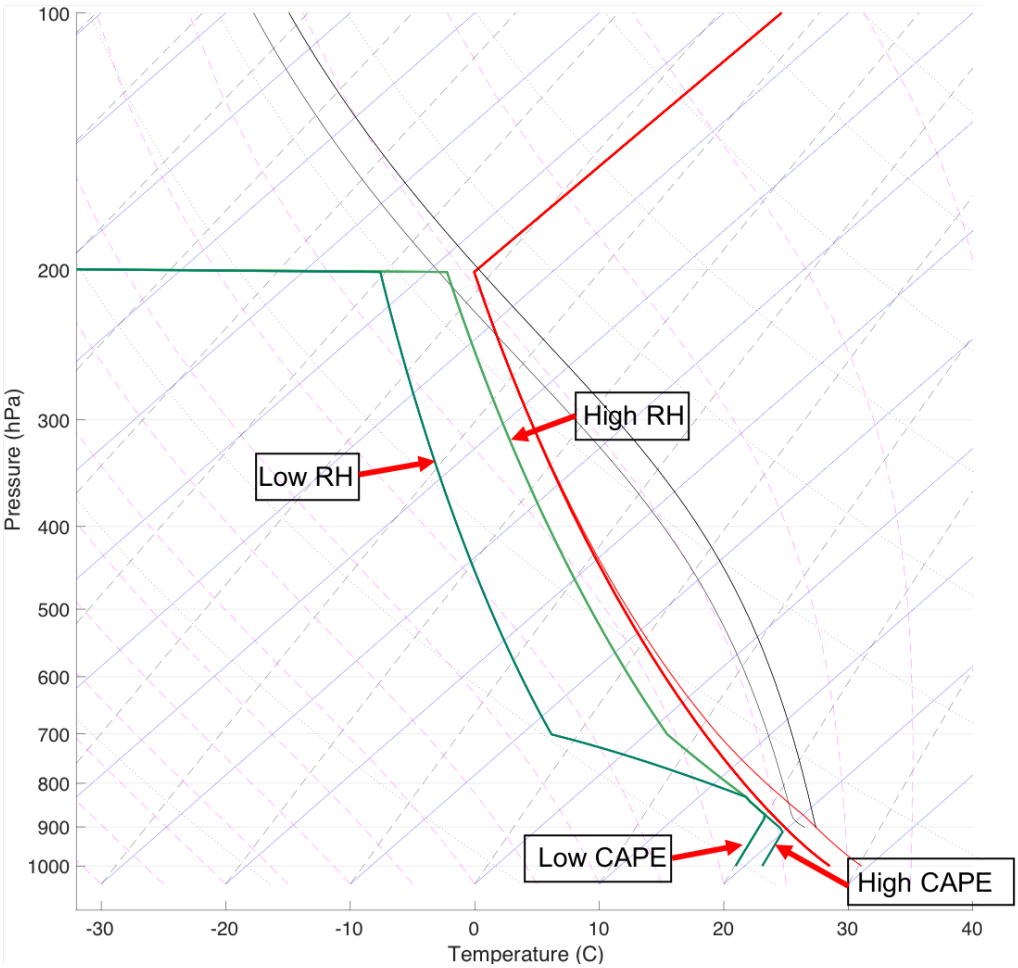

Skew *T* log *p* diagram depicting the temperature and moisture profiles used in the CM1 domain. Thin red line represents T_v of initial environment. Bold red line represents T of initial environment. Solid black line represents the temperature of a lifted air parcel with average properties of lowest 1 km of atmosphere. Green lines represent dewpoint and associated moisture values (dark green = lower values, light green = higher values). Tilted solid lines are isotherms, long dashed lines are moist adiabats, and short dashed lines are dry adiabats.

Figure 1. WK82 Environmental Sounding. Source: Weisman and Klemp (1982)

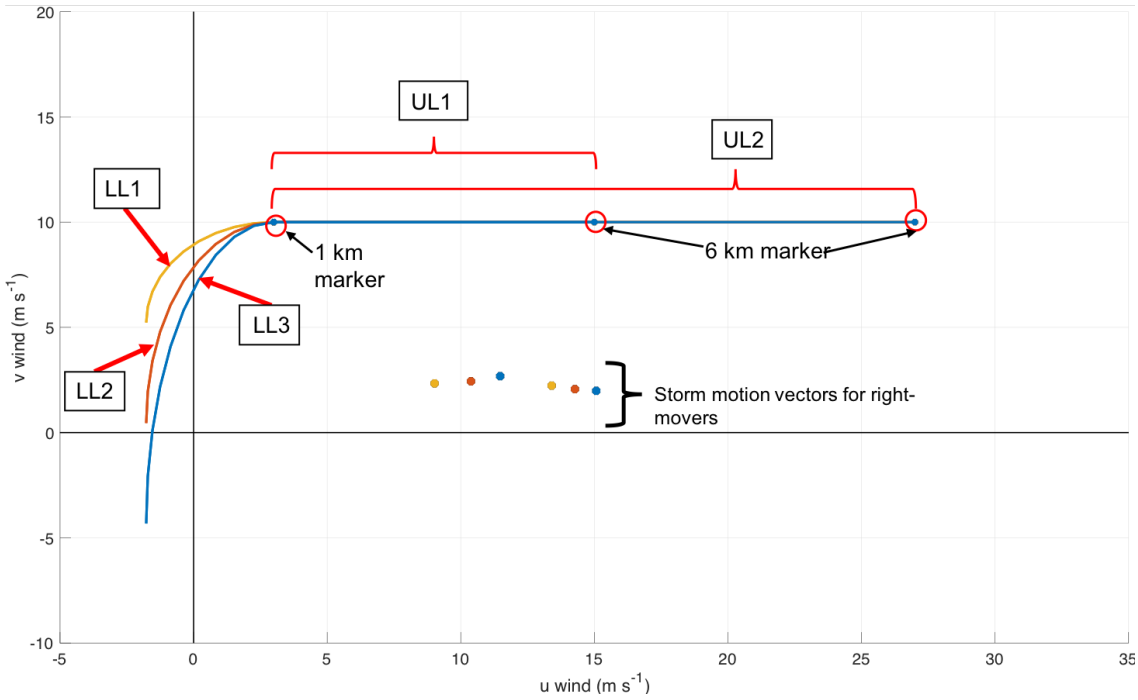

Hodograph depicting the wind profile used within the CM1 domain. Different low-level wind shear values represented by length/color of line with the lowest value (LL1) as short/yellow, the middle value (LL2) as middle/red, and the highest value (LL3) as long/blue. Upper-level wind shear values are represented as the length of the straight-line section with the lowest value (UL1) as the shortest line section and the highest values (UL2) as the longest line section. Multi-colored dots represent Bunkers et al. (2000) estimated storm motion vectors for right movers. U-wind on x-axis. V-wind on y-axis.

Figure 2. Environmental Hodograph. Source: Rotunno and Klemp (1982)

To test the sensitivity of supercell behavior to CAPE, relative humidity (RH), and variations of wind shear within the air column, a series of 24 numerical model runs were conducted with different variations in the quarter-circle wind profile and strength of shear as well as variations in the Convective Potential Available Energy (CAPE) and relative humidity (RH) parameters. The quarter-circle wind profile was modified by two independent methods. First, three separate values for the low-level wind shear were derived by multiplying the 0–1 km values of the original quarter-circle profile by 0.5, 0.75, and 1 (hereafter "LL1," "LL2," and "LL3"). In combination with the low-level shear, two values of upper-level shear (1-6 km) were assigned by multiplying the 0–6 km values of the original quarter-circle profile by 0.75 and 1 (hereafter "UL1" and "UL2"). Each of these variations were combined for a total of 12 base wind profiles. Two different RH values of

42.5 % (hereafter “dry,” RH1) and 85 % (hereafter “moist,” RH2) and above 3 km were used to evaluate the sensitivity of results to RH. In addition, two different values of boundary-layer moisture of 14 g kg^{-1} (1 km mean CAPE of 1729 J kg^{-1}, hereafter CAPE1) and 16 g kg^{-1} (1 km mean CAPE of 2744 J kg^{-1}, hereafter CAPE2) were also used in the WK82 sounding to test the sensitivity of storm evolution to boundary layer moisture and CAPE. Each of these moisture parameters were combined within the aforementioned base wind models for a model population of 24 independent runs, each of which labeled reflecting the variables used. For example, a model run with the LL1, UL1, CAPE1, and RH1 parameters is referred to as LL1_UL1_CAPE1_RH1.

Table 2. Model Run Break Down with Associated Label

Run Number	Title
1	LL1_UL1_CAPE1_RH1
2	LL1_UL1_CAPE1_RH2
3	LL1_UL1_CAPE2_RH1
4	LL1_UL1_CAPE2_RH2
5	LL1_UL2_CAPE1_RH1
6	LL1_UL2_CAPE1_RH2
7	LL1_UL2_CAPE2_RH1
8	LL1_UL2_CAPE2_RH2
9	LL2_UL1_CAPE1_RH1
10	LL2_UL1_CAPE1_RH2
11	LL2_UL1_CAPE2_RH1
12	LL2_UL1_CAPE2_RH2
13	LL2_UL2_CAPE1_RH1
14	LL2_UL2_CAPE1_RH2
15	LL2_UL2_CAPE2_RH1
16	LL2_UL2_CAPE2_RH2
17	LL3_UL1_CAPE1_RH1
18	LL3_UL1_CAPE1_RH2
19	LL3_UL1_CAPE2_RH1
20	LL3_UL1_CAPE2_RH2
21	LL3_UL2_CAPE1_RH1
22	LL3_UL2_CAPE1_RH2
23	LL3_UL2_CAPE2_RH1
24	LL3_UL2_CAPE2_RH2

C. ANALYSIS STRATEGIES

Each of the 24 runs produced scenarios that included supercells that made the transition to an MCS and those that failed to do so. An analysis was conducted of each storm's simulated radar reflectivity (dBz). Simulated radar reflectivity was used because of its ability to represent rain rate, and to maintain consistency with past studies that have looked at radar imagery (NOAA, 2009). According to the Radar Images: Reflectivity page hosted by NOAA (https://w1.weather.gov/glossary/index.php?letter=d; 2019), values of 20 dBz indicate falling precipitation and values of 40 dBz represent areas of moderate rainfall. Therefore, for this paper, areas of >40 dBz denote where the storm has become fully developed, and the size of this >40 dBz area will determine when the supercell has fully transitioned into an MCS. The focus on areas of > 40 dBz area as an indicator for MCS transition instead of the size of the cloud shield as annotated by Maddox (1980) stems from the understanding that severe weather typically occurs with the strongest updrafts (Gallus 2008). A supercell thunderstorm is considered to have transitioned into an MCS when the area of >40 dBz reaches and sustains an area measuring greater than 100 km for the remainder of the model run. The decision of 100 km being the area criteria is based on the definition of an MCS found in (Cotton et al. 1989), that an MCS is orders of magnitude greater than a single supercell thunderstorm, and that a single nonsupercell convective updraft width averages 1–3 km (Hernandez-Deckers and Sherwood 2016, Table 3) and supercell updrafts range from 5–10 km in diameter (Peters et al. 2019). An area of 100 km is 1–2 orders of magnitude greater, making it an acceptable marker for MCS transition. In order to accurately measure the area of significant updraft, MATLAB's "ellipse fit" function is used to create a border around all grid points measuring >40 dBz. This region-fitted ellipsoid changes size in sync with said region as the model run progresses through all remaining time steps. Simultaneously, the length of the semi-major axis is recorded and used as a determining factor of MCS transition. Once the length of the semi-major axis of the fitted ellipsoid representing the region of >40 dBz reaches a magnitude of 100 km, the super cell thunderstorm is considered to have completed its transition into an MCS. A version of the above analysis is also applied to the measurement of the resulting cold pool of each system. The same ellipsoid fitting technique is employed to measure and record

areas where the surface potential temperature perturbation reaches differences of -3°K or greater from the original model temperature. This temperature criterion was chosen to ensure that enough temperature distinction existed to identify the cold pool boundary for analysis. Total vertical mass flux is calculated at 5 km above ground level (AGL) for every time step and then analyzed in the form of a time series. Vertical mass flux relates to vertical moisture flux and correlates with precipitation production.

THIS PAGE INTENTIONALLY LEFT BLANK

III. RESULTS

For each of the model runs, the rate at which severe convection organized into an MCS was analyzed through the evolution of simulated radar reflectivity. Various physical characteristics were required to determine rate of convection organization during each stage of the system's development. In order for a storm to be considered a supercell, distinct patterns of development such as a hook echo, a v-signature in the forward flank precipitation, and a low-level updraft helicity maximum were needed with either the right, left, or both flanks sustaining areas of >40 dBz for the remainder of the model run or until MCS transition occurred. MCS transition was considered complete when one continuous area of >40 dBz spanned over 100km in the horizontal and then remained over 100km wide for the remainder of the model run. Of the 24 total model runs, 21 successfully created a supercell thunderstorm with radar reflectivity >40 dBz displayed as simulated radar reflectivity, and 11 of those supercell thunderstorms completed the transition into an MCS. Examples of this MCS transition can be seen in Figure 3.

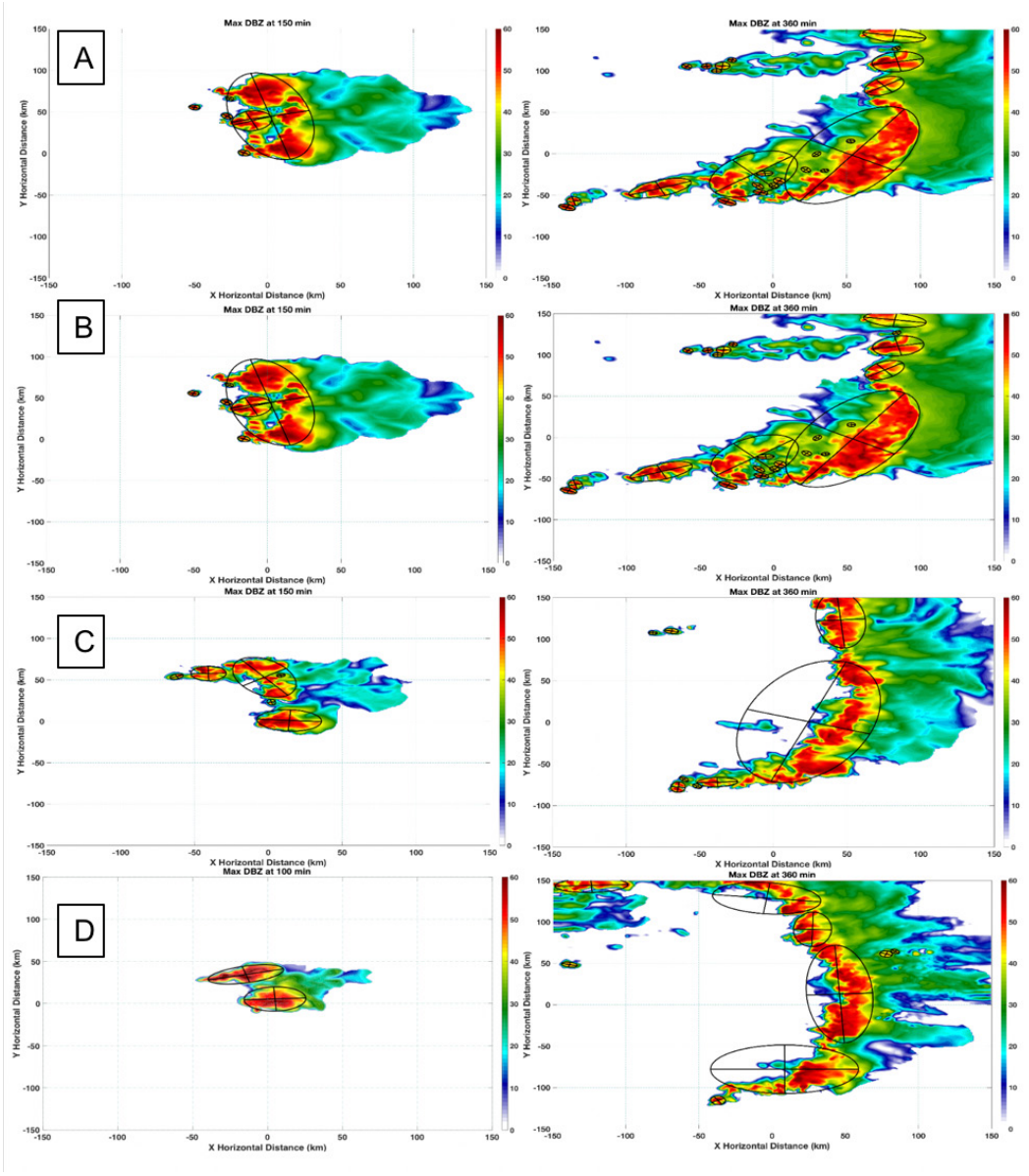

Left panel displays initial supercell thunderstorm. Right panel displays initial supercell thunderstorm after MCS transition. (A) LL1_UL1_CAPE2_RH2. (B) LL1_UL2_CAPE2_RH2. (C) LL2_UL2_CAPE2_RH1. (D) LL3_UL2_CAPE2_RH1. Shading colors depict simulated radar reflectivity (dBz). Both x- and y-axis depict distance (km).

Figure 3. Radar Reflectivity Comparison

For analysis, each model run was categorized with respect to three scenarios, no supercell, supercell but no MCS, and supercell and MCS. After all model runs were

characterized, a deeper look at the common environmental elements of each group was conducted.

When investigating the three scenarios which failed to even create the initial supercell thunderstorm, two commonalities were observed. In each of the three scenarios, the area of >40 dBz only persisted for an average of 100 min as seen in Fig 4. and each model run contained the lowest values of upper level shear, CAPE, and relative humidity (UL1_CAPE1_RH1) combined. In each sequential model run, the value of low-level wind shear increased from LL1 to LL2 to LL3 with no perceivable effect on the scenario development, meaning that low-level wind shear did not seem to affect this scenario. Each run produced small areas of > 40 dBz convection; however, none of the runs were able to sustain this small area of convection for longer than 180 mins.

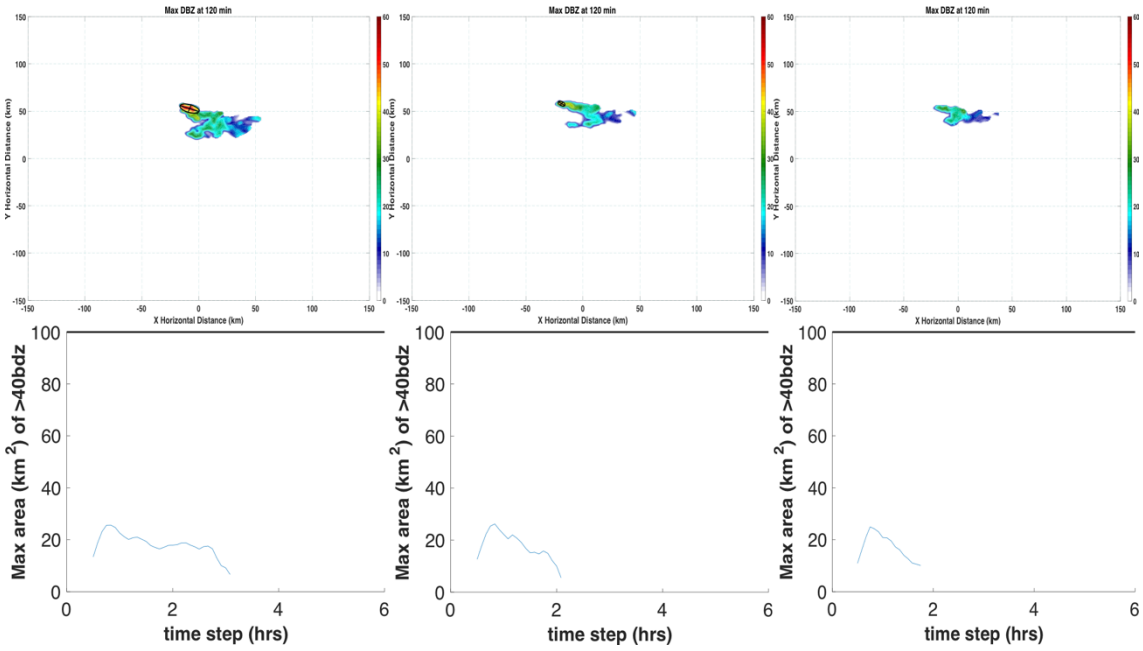

Right panel is LL1_UL1_CAPE1_RH1 run, middle panel is LL2_UL1_CAPE1_RH1 run, and left panel is LL3_UL1_CAPE1_RH1 run. Top row: x- and y-axis denote distance (km). Shading colors depict simulated radar reflectivity (dBz). Bottom row: x-axis represents time (hrs). Y-axis represents max area of >40 dBz convectivity.

Figure 4. Radar Reflectivity and Associated Time Series of Non-Supercell Scenarios

The second grouping of model runs analyzed consisted of those that were successful in creating the initial supercell thunderstorm but failed to trigger the transition of said thunderstorm into an MCS. Of the 21 scenarios which created a supercell, ten fell into "Supercell, but not MCS" category. Again, several commonalties of the environmental components across all these model runs came to light. First, all scenarios had the lowest CAPE values, CAPE1, (the two exception cases will be addressed later) which is a trait shared with the non-supercell cases. At face value, this supports the hypothesis that CAPE is the primary driver in the MCS development in that lower CAPE values resulted in a low incidence of MCS development. However, the separating factor seems to be a combination of elevated wind shear values or relative humidity. Any individual case that contained LL1 also contained UL2, any case that contains UL1 also contains either LL2 or LL3, and the cases with both LL1 and UL1 also contained RH2. All combination cases appear to, individually, be just enough of an environmental edge to tip the non-supercell case into a successful supercell case, but not enough to trigger the MCS transition. The two previously mentioned exceptions were cases LL1_UL2_CAPE2_RH1 and LL2_UL1_CAPE2_RH1. Both possess CAPE2 and not CAPE1 yet still failed to initiate MCS transition. It is proposed that each of these scenarios were showing signs of MCS transition towards the end of the model run, and would have completed transition should the run have continued for at least an extra 30 mins. Their specific convection area of >40 dBz time series plots can be seen in Figure 5. It is suspected that the presence of stronger low-level and/or deep-layer shear may have dampened the transition process, forcing more time before the CAPE2 value was able to trigger an MCS transition; however, this will require further investigation to confirm.

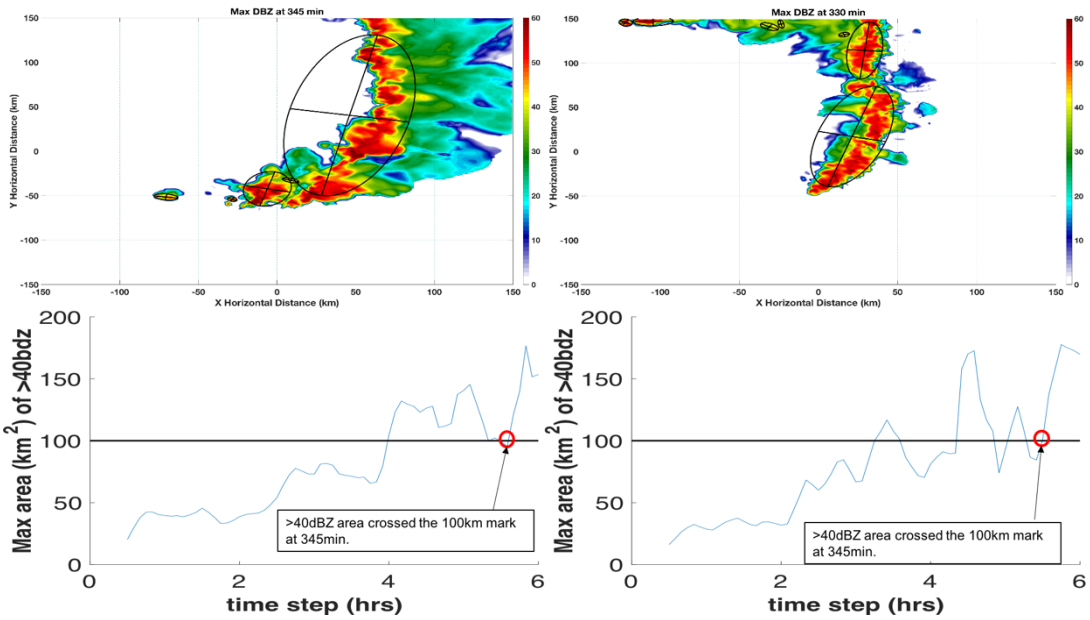

Right panel is LL1_UL2_CAPE2_RH1 run and left panel is LL2_UL1_CAPE2_RH1 run. Top row: x- and y-axis denote distance (km). Shading colors depict simulated radar reflectivity (dBz). Bottom row: x-axis represents time (hrs). Y-axis represents max area of >40 dBz convectivity.

Figure 5. Radar Reflectivity and Associated Time Series of Non-Transitional Supercell Scenarios

The remaining grouping of model runs to be examined where those that both created a sustained supercell thunderstorm and also triggered the transition into an MCS. Of the 24 total runs studied throughout this experiment, only 11 fell into this category. The glaring environmental commonality between each of these specific cases was the presence of the highest value of CAPE, CAPE2, which was different than the other scenarios which had the lowest value of CAPE. This again supports the paper's main hypothesis in that the highest CAPE values were associated with the highest incidence of MCS development. Throughout the 11 transition cases various combinations of LL1, LL2, LL3, UL1, UL2, RH1, and RH2 were investigated, similar to the combinations seen in the non-supercell and supercell cases; however, none of the various environmental value combinations appear to have an effect as to whether the MCS transition occurs. This suggests that MCS development depends mainly on the thermodynamic factors, rather than on the details of an environmental wind profile. The only exception was run LL1_UL1_CAPE1_RH2

which was able to complete the MCS transition with CAPE1 value. This CAPE value alone should determine that this case would create a non-transitioning supercell thunderstorm; however, again, the effects of wind shear can be observed but in the opposite function as noted before. It is suspected that this model run was only successful in completing the transition due to the presence of LL1 and UL1, meaning that very small wind shear in combination of the smaller CAPE value allowed a sufficiently large cold pool and related MCS to develop.

Figures 6 and 7 show all model runs in comparison to each other and their representative characteristics. Figure 6 graphically shows the result that CAPE is the main environmental factor that supports supercell transition into an MCS while there is no perceived change when comparing the two wind shear elements. Figure 7 displays the resulting three groups of model runs of non-supercell, supercell but no transition, and successful MCS transition respectfully. By organizing the results in this manor, it is easy to again see that CAPE is the dominant factor in determining the likelihood of supercell transition into an MCS.

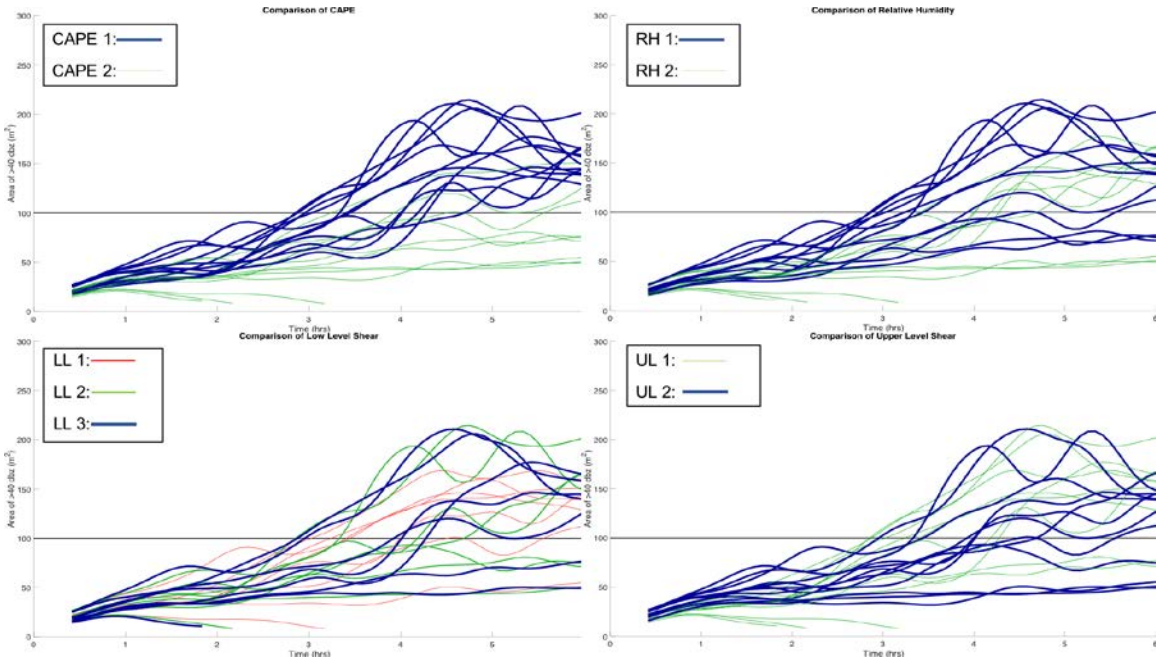

Time series depiction of growth of >40 dBz radar reflectivity area against independent environmental factors. The x-axis is time (hrs). The y-axis is area (m^2). Upper left panel: Comparison with respect to CAPE. Upper right panel: Comparison with respect to relative humidity. Lower left panel: Comparison with respect to low-level shear. Lower right panel: Comparison with respect to upper-level wind shear. Blue lines represent highest values of respective variable. Green lines represent lowest value of respective variable unless red is present, then green represents the middle values. If present, red lines represent the lowest of three values of the respective variable.

Figure 6. Comprehensive Comparison of All Environmental Factors Related to Radar Reflectivity Across All Model Runs.

Cases that did NOT create a supercell:
LL1 UL1 CAPE1 RH1
LL2 UL1 CAPE1 RH1
LL3 UL1 CAPE1 RH1
Cases that did create a supercell, but NOT an MCS:
★ LL1 UL2 CAPE2 RH1
LL1 UL2 CAPE1 RH2
LL1 UL2 CAPE1 RH1
★ LL2 UL1 CAPE2 RH1
LL2 UL1 CAPE1 RH2
LL2 UL2 CAPE1 RH2
LL2 UL2 CAPE1 RH1
LL3 UL1 CAPE1 RH2
LL3 UL2 CAPE1 RH2
LL3 UL2 CAPE1 RH1
Cases that created an MCS:
LL1 UL1 CAPE2 RH2
LL1 UL1 CAPE2 RH1
★ LL1 UL1 CAPE1 RH2
LL1 UL2 CAPE2 RH2
LL2 UL1 CAPE2 RH2
LL2 UL2 CAPE2 RH2
LL2 UL2 CAPE2 RH1
LL3 UL1 CAPE2 RH2
LL3 UL1 CAPE2 RH1
LL3 UL2 CAPE2 RH2
LL3 UL2 CAPE2 RH1

Breakdown of the 24 model runs into three distinctive cases: no supercell development, supercell formation but no MCS transition, and successful supercell transition into an MCS. Red rectangles highlight CAPE variables in both cases that only created a supercell (CAPE1) and those that transitioned into an MCS (CAPE 2). Red Stars annotate exception cases to the respective case CAPE value rule.

Figure 7. Three Model Run Resultant Cases

Cold pool analysis was conducted by measuring the area of >3°C surface temperature perturbations at each time step and then examined as a time series. Of the 21 model runs that successfully created a supercell thunderstorm, the cold pool growth rate proceeded the >40 dBz area in all but three cases. For the group of model runs that produced a supercell thunderstorm that did not successfully transition into an MCS, the cold pool area reached the 100 km MCS threshold between 30–56 mins before the convective area surpassed the MCS threshold. Two model runs in this group did produce a cold pool that did not cross the MCS threshold, LL2_UL2_CAPE_1_RH1 and LL3_UL2_CAPE1_RH1 and are two of the three aforementioned cold pool exception cases. For the group of 11

model runs whose supercell thunderstorms completed the transition into an MCS, the cold pool crossed the MCS threshold between 35–60 mins. The time between each supercell's cold pool reaching the MCS threshold and the associate supercell initiating its transition into an MCS ranges from 4–19 mins with 6 cases below 10 mins and 4 cases ranging from 10–19 mins. The one exception case for this groups is model run LL2_UL1_CAPE2_RH2 whose >40 dBz area proceed the cold pool in reaching the MCS threshold by 2 mins. All results remain consistent with results of previous research relating cold pool formations to a supercell thunderstorm's transition into an MCS. Similar trends in cold pool extent with respect to the particular run's CAPE value were similar to those deduced in the >40dBz analysis, specifically that cases with higher CAPE values also exhibited larger cold pool extents.

Total mass flux was calculated across the whole domain as the total mass flowing across the horizontal 5km boundary. Results were consistent with those of the >40 dBz analysis. For the three cases that failed to create a supercell thunderstorm, total mass flux rates never increased higher than 1 $Tgs^{-}1$, for the cases that created a supercell thunderstorm but did not transition into an MCS the total mass flux rates ranged from 2–7 Tgs^{-1}, and for the cases where the supercell thunderstorm successfully transitioned into an MCS the total mass flux rates range from 3–12 Tgs^{-1}. All of these case comparisons can be seen in Figure 8. This correlation of higher rates of mass flux correlate closely with previous research linking higher rates of total mass flux with supercell thunderstorm transition into an MCS. Overall, we suggest that the mass flux rates were higher in the high CAPE environments because of greater updraft buoyancy, buoyant accelerations, and vertical velocities. These stronger updrafts apparently facilitated larger precipitation production, larger cold pools, and ultimately faster MCS growth than in the case of lower environmental CAPE.

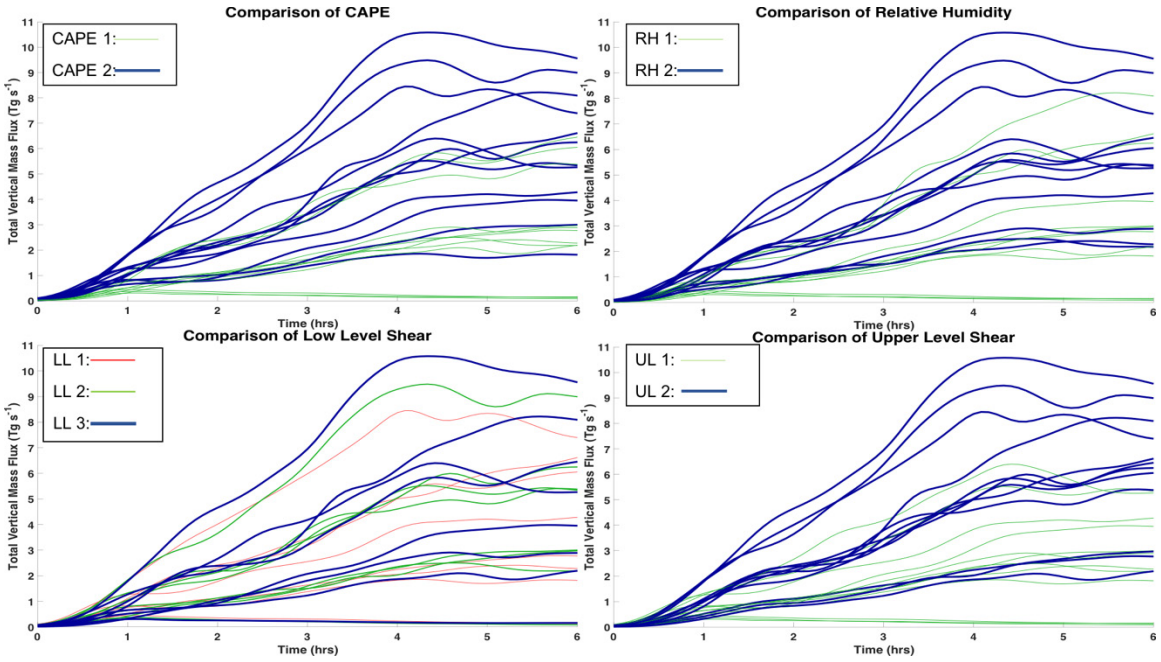

Time series depiction of growth of total mass flux across 5 km AGL against independent environmental factors. The x-axis is time (hrs). The y-axis is area (m^2). Upper right panel: Comparison with respect to relative humidity. Lower left panel: Comparison with respect to low-level shear. Lower right panel: Comparison with respect to upper-level wind shear. Blue lines represent highest values of respective variable. Green lines represent lowest value of respective variable unless red is present, then green represents the middle values. If present, red lines represent the lowest of three values of the respective variable.

Figure 8. Comprehensive Comparison of All Environmental Factors Related to Total Mass Flux across All Model Runs

Coriolis force was ignored for all model runs due to the short duration of the experiment (6 hours); however, to allay any suspicions that Coriolis force might possibly impact any of the results, several of the model runs were repeated with the Coriolis force applied to model perturbation variables only. There were no distinguishable differences in the results of the these runs when compared to corresponding "No Coriolis" model run, as seen in Figure 9.

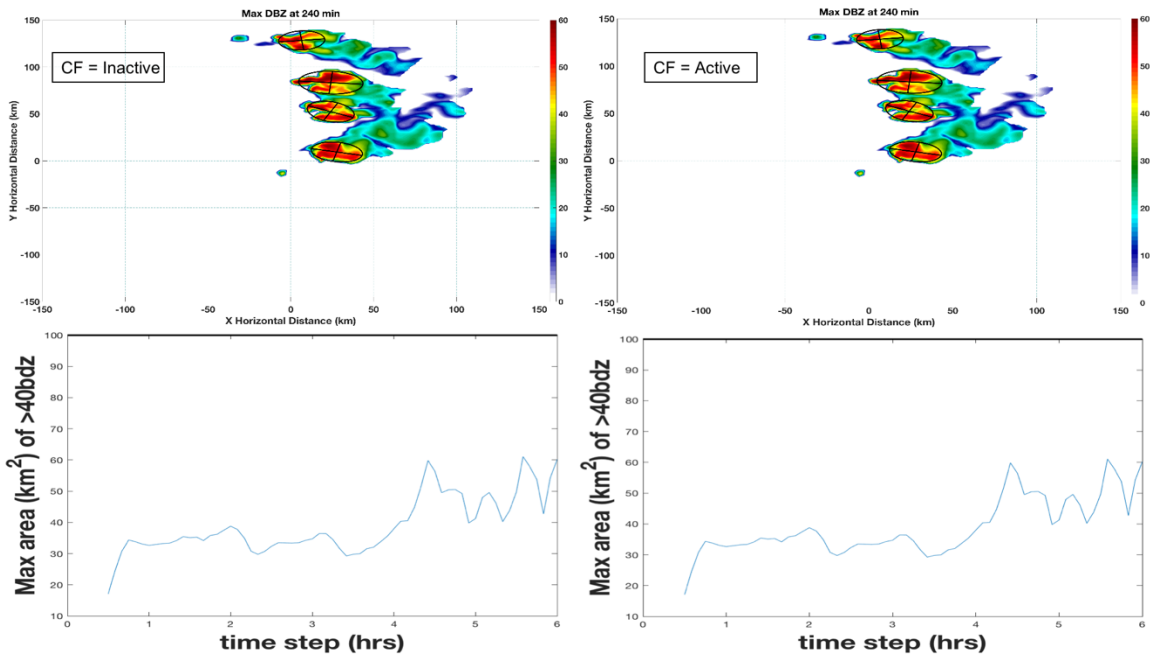

Comparison of model run LL1_UL2_CAPE1_RH1 with Coriolis force parameters inactive (left) and active (right). Top row: x- and y-axis denote distance (km). Shading colors depict simulated radar reflectivity (dBz). Bottom row: x-axis represents time (hrs). Y-axis represents max area of >40 dBz convectivity.

Figure 9. Investigation into Coriolis Force on Results

THIS PAGE INTENTIONALLY LEFT BLANK

IV. CONCLUSION

This paper investigated the relationship between different environmental factors and their impacts to the transition of a supercell thunderstorm into an MCS. Environmental factors studied include low-level wind shear (0-1 km), upper-level wind shear (0-6 km), convective available potential energy (CAPE), and relative humidity. The hypothesis considered states that MCS transition is primarily forced by the CAPE and relative humidity values rather than the environmental wind shear profile.

To test this hypothesis, numerical simulations were run from initially horizontally homogenous domain. Then each of the four environmental factors were systematically varied to produce unique "atmospheres" wherein conditions for supercell thunderstorm formation were initialized. Both CAPE and relative humidity were assigned a "high" and "low" value, the ideal low-level wind shear profile was multiplied by factors of 0.5, 0.75, and 1, and the ideal upper-level wind shear profile was multiplied by factors of 0.75 and 1. In total, 24 individual model runs were completed, and the results examined through the comparison of both the resulting radar reflectivity and amount of vertical mass flux at the 5 km horizontal boundary. The results derived from these model runs are described as follows:

- In cases where supercell thunderstorms developed and completed the transition into an MCS, the highest CAPE value was the most distinct factor in all but one case. All other variations of low-level and upper-level wind shear values were investigated with no observable contribution to supercell transition.
- In cases where a supercell thunderstorm developed but did not initiate MCS transition, the lowest value of CAPE was present; however, each case noticeably contained an elevated value of either upper-level wind shear or relative humidity. In seven of the ten cases the highest value of upper-level wind shear was present with varying patterns of relative humidity values. However, in each of the 3 remaining cases exhibiting the lowest value of upper-level wind shear, the highest value of relative humidity was present. It is thought that the

elevated value of relative humidity contributed to less precipitation evaporation. This lack of evaporation then led to more rain at the surface and a stronger cold pool that provided the extra push the environment needed to produce a supercell thunderstorm in the cases lacking of sufficient upper-level wind shear. Various combinations of low-level wind shear values were also tested with no observable contributions.

- In cases were no supercell thunderstorm developed, lowest values of CAPE, relative humidity, and upper-level shear were present. Again, all three values of low-level wind shear were evaluated with no observable effect.
- Interestingly, the three exceptions to the CAPE value predictor of MCS transition, one that successfully transitioned into an MCS and two that created a supercell thunderstorm but did not create an MCS, hint at a relationship between the presence of wind shear and the delayed development of a supercell thunderstorm as well as the supercell's transition into an MCS.
- Comparison of vertical mass flux throughout all cases mirror the above results found through comparison of system radar reflectivity, highlighting that cases possessing the highest CAPE values were the cases that initiated the transition into an MCS and that when making a distinction between MCS and non-MCS systems, differing wind shear values and combinations had no observable effect on model run results.
- The cases that successfully created an MCS also exhibited the highest values of vertical mass flux. It is suspected that the larger vertical mass flux in the MCS cases contributed to more rainfall, leading to a more widespread and intense cold pool, which then led to faster upscale growth.

The results of this study can be employed in refining the forecasting techniques for MCS transition, increasing the public's ability to prepare for the correct severe weather threat. With supercell thunderstorms there is the threat of lightning, hail, and tornados. With the MCS, the threat shifts to that of widespread flash flooding with a dramatic decrease of tornadic probability. Future studies should include investigations into a value

range for CAPE, relative humidity, and upper-level wind shear that denotes when a supercell will transition into an MCS, determining the exact role that wind shear plays in the dampening of supercell development, investigating the effect of multiple supercell thunderstorms in the same domain on both the probability and rate of transition into an MCS in order to more accurately represent what is observed in nature, and investigating the dynamic relationship between vertical mass flux and MCS transition.

THIS PAGE INTENTIONALLY LEFT BLANK

LIST OF REFERENCES

Brooks, H.E., Doswell III, C.A., and Cooper, J., 1994, On the Environments of Tornadic and Nontornadic Mesocyclones, Wea. *Forecasting*, 9, 606–618.

Coniglio, M.C., H.E. Brooks, S. J. Weiss, and S. F. Corfidi, 2007: Forecasting the maintenance of quasi-linear mesoscale convective systems. *Wea. Forecasting*, 22, 556–570.

Coniglio, M.C., and S.F. Corfidi, 2006: Forecasting the Speed and Longevity of Severe Mesoscale Convective Systems, Preprints, Severe Local Storms Symposium, Amer. Meteor. Soc., Atlanta, GA, CD-ROM.

Coniglio, M.C., J.Y. Hawang, and D. J. Stensrud, 2010: Environmental Factors in the Upscale Growth and Longevity of MCSs Derived from Rapid Update Cycle Analyses. *Mon. Wea. Rev*., 138, 3514–3539.

Cotton, W.R., M.S. Lin, R.N. McAnelly, and C.J. Tremback, 1989, A Composite Model of Mesoscale Convective Complexes, *Amer. Meteor. Soc*., 117, 765–783.

Davies-Jones, R., 1984: Streamwise vorticity: The Origin of Updraft Rotation in Supercell Storms. *J. Atmos. Sci*., 41, 2991–3006.

Fritsh, J.M, and Forbes G.S., 2001, Mesoscale Convective Systems, Severe Convective Storms, C.A. Doswell, III, Ed., *Am Met Soc*, 323–357.

Fritsh, J.M., R. J. Kane, and C.R. Chelius, 1986, The Contribution of Mesoscale Convective Weather Systems to the Warm-Season Precipitation in the United States, *J. Appl. Meteor. Climatol*., 25, 10, 1333–1345, 10.1175/1520-0450(1986)025<1333:TCOMCW>2.0.CO;2.

Gallus, W.A.J., N.A. Snook, and E. V. Johnson, 2008: Spring and Summer Severe Weather Reports over the Midwest as a Function of Convective Mode: A Preliminary Study. *Wea. Forecasting*, 23, 101–113.

Grant, L.D. and S.C. van den Heever, 2014: Microphysical and Dynamical Characteristics of Low-Precipitation and Classis Supercells. *J. Atmos. Sci*., 71, 2604–2624, https://doi.org/10.1175/JAS-D-13-0261.1.

Gropp, M.E. and C.E. Davenport, 2018: The Impact of the Nocturnal Transition on the Lifetime and Evolution of Supercell Thunderstorms in the Great Plains. *Wea. Forecasting*, 33, 1045–1061, https://doi.org/10.1175/WAF-D-17-0150.1.

Hernandez-Deckers, D., and S.C. Sherwood, 2016, A Numerical Investigation of Cumulus Thermals, *J. Atmos. Sci*., 73, 10, 4117–4136, 10.1175/JAS-D-15-0385.

Hitchens, N.M., and H E. Brooks, 2013: Preliminary Investigation of the Contribution of Supercell Thunderstorms to the Climatology of Heavy and Extreme Precipitation in the United States. *Atmos. Res*., 123, 206–210.

NCAR, 2019: Answers to Frequently Asked Questions about CM1. Accessed 21 August 2019, http://www2.mmm.ucar.edu/people/bryan/cm1/faq.html.

NOAA, 2009: Weather Glossary: D's. Accessed 21 August 2019, https://w1.weather.gov/glossary/index.php?letter=d

NOAA, 2019: Radar Images: Reflectivity. Accessed 21 August 2019, https://www.weather.gov/jetstream/refl

Maddox, R. A., 1980, Mesoscale Convective Complexes, Bull. *Amer. Meteor. Soc*., 61, 11, 1374–1387, 10.1175/1520-0477(1980)061<1374:MCC>2.0.CO;2.

Markowski, P.M., 2007, *Supercell Thunderstorms, Atmospheric Convection: Research and Operational Forecasting Aspects*, D.B. Giaiotti, R. Steinacker, and F. Stel, Eds., SpringerWien, New York, 29–43.

Markowski, P.M., 2007a, *Convective Storm Initiation and Organization, Atmospheric Convection: Research and Operational Forecasting Aspects*, D.B. Giaiotti, R. Steinacker, and F. Stel, Eds., SpringerWien, New York, 23–28.

Markowski, P.M. and Y.P Richardson, 2014, The Influence of Environmental Low-Level Shear and Cold Pools on Tornadogenesis: Insights from Idealized Simulations. *J. Atmos. Sci*., 71, 242–275, https://doi.org/10.1175/JAS-D-13-0159.1.

McAnelly, R.L., and W.R. Cotton, 1989, The Precipitation Life-Cycle of Mesoscale Convective Complexes Over the Central United States. *Mon. Wea. Rev*., 117, 4, 784–808, 10.1175/1520-0493(1989(117<0784:TPLCOM>2.0.CO;2.

Morrison, H., 2017: An Analytic Description of the Structure and Evolution of Growing Deep Cumulus Updrafts. *J. Atmos. Sci*., 74, 809–834, https://doi.org/10.1175/JAS-D-16-0234.1.

Nielsen, E.R., G.R Herman, R.C. Tournay, J.M. Peters, and R.S. Schumacher, 2015: Double Impact: When Both Tornadoes and Flash Floods Threaten the Same Place at the Same Time. *Wea. Forecasting*, 30, 1673–1693, http://doi.org/10.1175/WAF-D-15-0084.1.

Parker, M.D., 2014, Composite VORTEX2 Supercell Environments from Near-Storm Soundings, *Mon. Wea. Rev*., 142, 508–529, https://doi.org/10.1175/WMR-D-00167.1.

Peters, J.M., and R.S. Schumacher, 2014: Objective Categorization of Heavy-Rain-Producing MCS Synoptic Types by Rotated Principal Component Analysis. *Mon. Wea. Rev*., 142, 1716– 1737.

Peters, J.M., and R.S. Schumacher, 2015a: Mechanisms for Organization and Echo Training in a Flash-Flood-Producing Mesoscale Convective System. *Mon. Wea. Rev*., 143, 1058–1085.

Peters, J.M., and R.S. Schumacher, 2016: Dynamics Governing a Simulated Mesoscale Convective System with a Training Convective Line. *J. Atmos. Sci*., 73, 2643–2664.

Peters, J.M., C.J. Nowotarski, and H. Morrison, 2019: The Role of Vertical Wind Shear in Modulating Maximum Supercell Updraft Velocities. *J. Atmos. Sci.,* 76, 3169–3189, https://doi.org/10.1175/JAS-D-19-0096.1.

Proctor, F.H., 1989: Numerical Simulations of an Isolated Microburst. Part II: Sensitivity Experiments. *J. Atmos. Sci.,* 46, 2143–2165, https://doi.org/10.1175/1520-0469(1989)046<2143:NSOAIM>2.0.CO;2.

Rasmussen, E.N., and R.B. Wilhelmsen, 1983: Relationships between Storm Characteristics and 1200 GMT Hodographs, Low Level Shear, and Stability. Preprints, 13th Conf. on Severe Local Storms, Tulsa, OK, Amer. Meteor. Soc., J5-J8.

Rotunno, R., and J. B. Klemp, 1982: The Influence of the Shear-Induced Pressure Gradient on Thunderstorm Motion. *Mon. Wea. Rev*., 110, 136–151, doi:http://dx.doi.org/10.1175/ 1520–0493(1982)110h0136:TIOTSIi2.0.CO;2.

Smith, J.A., M.L. Baeck, Y. Zhang, and C. A. D. III, 2001: Extreme Rainfall and Flooding from Supercell Thunderstorms. *J. Hydro. Met*., 2, 469–489.

Thompson, R.L., R. Edwards, J.A. Hart, K L. Elmore, and P. Markowski, 2003: Close proximity soundings within supercell environments obtained from the Rapid Update Cycle. *Wea. Forecasting*, 18, 1243–1261, https://doi.org/10.1175/1520-0434(2003)018<1243:CPSWSE>2.0.CO;2.

Thompson, R L., C.M. Mead, and R. Edwards, 2007: Effective Storm-Relative Helicity and Bulk Shear in Supercell Thunderstorm Environments. *Wea. Forecasting*, 22, 102–115.

Thompson, R L., B.T. Smith, J S. Grams, A.R. Dean, and C. Broyles, 2012: Convective Modes for Significant Severe Thunderstorms in the Contiguous United States. Part II: Supercell and QLCS Tornado Environments. *Wea. Forecasting*, 27, 1136–1154.

Tollerud, E.I., and R.S. Collander,1993: Proceedings Paper, Mesoscale Convective Systems and Extreme Rainfall in the Central United States; Int. Symp. on Extreme Hydrological Events: Precipitation, Floods and Droughts; Yokohoma, Japan; Int Assoc Hydrol SCI, *Int Assoc Meteorol & Atmospher Phys, and UNESCO*; 11–19.

Weisman, M.L., 1992: The Role of Convectively Generated Rear-Inflow Jets in the Evolution of Long-Lived Mesoconvective Systems. *J. Atmos. Sci.,* 49, 1826–1847.

Weisman, M.L., 1993: The Genesis of Severe, Long-Lived Bow Echoes. *J. Atmos. Sci.,* 50, 645–670.

Weisman, M.L., and Klemp, J.B., 1984, The Structure and Classification of Numerically Simulated Convective Storms in Directionally Varying Wind Shears, *Mon. Wea. Rev*., 112, 2479–2498.

Weisman, M.L., and J.B. Klemp, 1982: The Dependence of Numerically Simulated Convective Storms on Vertical Wind Shear and Buoyancy. *Mon. Wea. Rev*., 110, 504–520, doi:http://dx.doi. org/10.1175/1520-0493(1982)110h0504:TDONSCi2.0.CO;2.

Weisman, M.L., and R. Rotunno, 2000: The Use of Vertical Wind Shear Versus Helicity in Interpreting Supercell Dynamics. *J. Atmos. Sci.,* 57, 1452–1472, doi:http://dx.doi.org/10.1175/ 1520–0469(2000)057h1452:TUOVWSi2.0.CO;2.

Weisman, M.L., and Rotunno, R., 2004: A Theory for Strong Long-Lived Squall Lines Revisited, *J. Atmos. Sci.,* 61, 361–382.

INITIAL DISTRIBUTION LIST

1. Defense Technical Information Center
   Ft. Belvoir, Virginia

2. Dudley Knox Library
   Naval Postgraduate School
   Monterey, California